JOURNAL OF GEOPHYSICAL RESEARCH, VOL. 86, NO. C7, PAGES 6451-6466, JULY 20, 1981

Field Observations of Surf Beat
1. Progressive Edge Waves

D. A. HUNTLEY

Department of Oceanography, Dalhousie University, Halifax, Nova Scotia, Canada

R. T. GUZA

Center for Coastal Studies, Scripps Institution of Oceanography, La Jolla, California

E. B. THORNTON

Department of Oceanography, Naval Postgraduate School, Monterey, California

Nineteen biaxial electromagnetic current meters have been used to determine the longshore and on/offshore structure of currents at surf beat periods (1–4 min). The sensors formed two linear arrays, a longshore array within the surf zone and an on/offshore array stretching from the shoreline to well beyond the breaker line. Analysis of the longshore current components yields a clear picture of progressive low-mode edge waves, with frequency-wave number dispersion relations which are in remarkably good agreement with predictions. Some separation of edge wave modes is found, with mode zero energy dominating in the frequency band 0.006 and 0.011 Hz and mode one between 0.015 and 0.025 Hz. On/offshore currents present a rather different picture which, while not inconsistent with the longshore currents, suggests that other sources of energy are also important to the on/offshore currents. These include standing edge waves probably formed by reflections at nearby Scripps Canyon, and motions which are nonresonantly forced by incoming wave groups.

INTRODUCTION

Since the initial observations of surf beat by *Munk* [1949] and *Tucker* [1950], the existence of a broad low frequency energy peak in spectra of wave motion close to the shore has been well documented. The range of periods associated with this peak is generally found to be about 40–300 s [*Munk*, 1949], though some observations suggest much narrower peaks within this range [*Huntley*, 1976].

Several possible sources of this low frequency energy have been discussed. *Munk* [1949] and *Tucker* [1950] interpreted their observations, taken several hundred meters offshore, as being due to mass transport shoreward under high incident wave groups, with the release of low frequency free waves at the break point, where the groups are destroyed by breaking. Tucker found that the maximum correlation between incident wave amplitude and low frequency motion was negative with a time lag which appeared to correspond to the travel time required for the low frequency motion to travel with the incident wave groups from the observation point to the break point and then propagate back seaward as a free wave. The negative correlation implies that high wave groups were correlated with troughs in the low frequency waves. *Longuet-Higgins and Stewart* [1962] subsequently showed that this observation agrees with the predicted second order forced waves under wave groups. The observed time lag implies that the seaward propagating free wave was larger than the incoming forced wave. However, *Hasselmann et al.* [1963] presented evidence that forced motion associated with nonlinear interaction between incident waves could explain the low frequency energy which they observed, without requiring any outgoing free waves. Thus ideas about the processes occurring at the breakpoint and the release of a seaward propagating low frequency wave, as indicated by the observations of Munk and Tucker, remain unresolved.

Copyright © 1981 by the American Geophysical Union.

Paper number 1C0556.
0148-0227/81/001C-0556$01.00

The suggestion that surf zone energy at surf beat frequencies is associated with progressive edge waves rather than forced waves appears to have originated with *Inman and Bowen* [1967]. In considering the generation of these edge waves, *Gallagher* [1971] extended the idea of forcing by incident wave groups to include the possibility of longshore variations in wave height if waves approach the shore at an oblique angle. Certain combinations of group frequency and longshore wave number can cause the resonant excitation of edge waves, the free wave modes trapped to the shoreline. *Bowen and Guza* [1978] clarified the physical processes involved in this resonant excitation of edge waves and concluded, on the basis of laboratory experiments, that the resonant edge wave response should be more important than nonresonant forced motion at surf beat frequencies. *Huntley* [1976] had previously shown field measurements from three sensors on a shore-perpendicular line which supported this idea. *Munk et al.* [1964] had also found that edge waves dominate the pressure field at a depth of 7 m for periods of 4–30 min but aliasing problems prevented a clear demonstration of the form of shorter period energy.

Low frequency free wave motion close to the shore can, in fact, take several forms. The edge waves measured by *Munk et al.* [1964] were progressive edge waves, with almost equal amounts of energy propagating northward and southward along the shore. However, it is possible that an obstruction or topographic change in the seabed could act as a reflector of these alongshore propagating waves and cause standing edge wave motion, with nodes and antinodes at fixed locations along the shore. Some field observations of surf beat energy do in fact suggest that such standing waves exist [*Huntley*, 1980*a*; *Wright et al.*, 1979] and topographic features such as crescentic bars require standing waves if they are indeed formed by edge waves [*Bowen and Inman*, 1971].

Edge waves are trapped to the coast with energy which decays assymptotically to zero at long distances from the

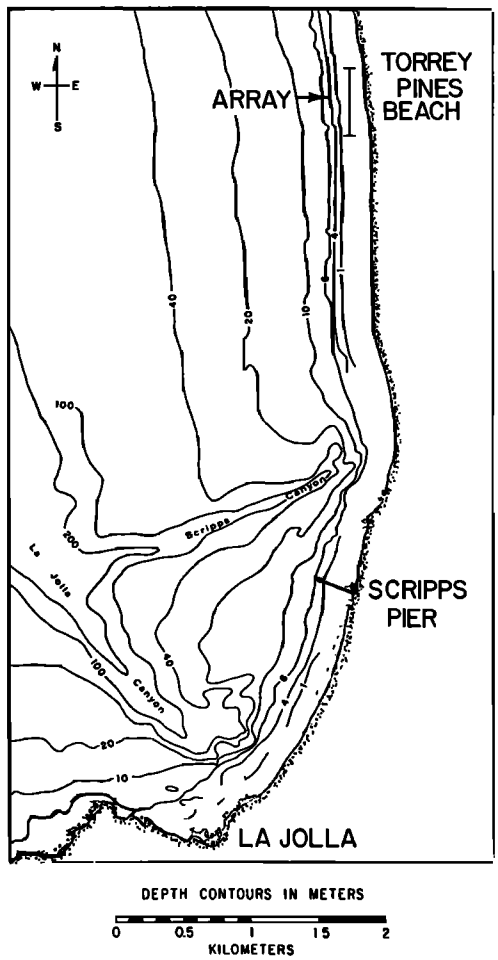

Fig. 1. Location of the longshore array of surf zone current meters at Torrey Pines Beach, La Jolla, California.

shoreline. *Ursell* [1952] showed that at any given frequency, such waves can only exist with longshore wave numbers greater than a critical 'cut-off' wave number which increases with increasing frequency. Free waves with longshore wave numbers less than the cut-off are leaky, radiating energy seaward, or conversely are the direct response of the nearshore zone to incoming wave energy of that frequency and longshore wave number. Unlike edge waves, which exist only at discrete longshore wave numbers (each corresponding to a different edge wave mode), these leaky free waves can take any longshore wave number in the continuum of wave numbers below the cut-off. *Munk et al.* [1964] found no evidence for these leaky waves in their observations. In view of the long periods of surf beat motion relative to normal incident wave periods, it seems unlikely that much of the observed energy is due to incoming free waves of surf beat period, but, as we have seen, seaward propagating free waves might be driven by nonlinear processes as incident wave groups reach the surf zone.

The purpose of this paper is to describe results of field measurements which allow us to assess, to some degree, the relative importance of these possible sources of surf beat energy. In particular, we show the first definitive evidence that progressive edge waves form an important component of surf beat energy. The data show, however, that other forms of energy are also important, contributing particularly to the on/offshore flows. Forced wave motion is undoubtedly present, but the evidence suggests that free edge waves which are standing in the longshore direction contribute significantly to this additional energy.

The Field Measurements

Field measurements were made at Torrey Pines Beach, San Diego, California (Figure 1), on November 20 and 21, 1978. The beach is particularly suitable for the present investigation being on a long, essentially straight coastline and having a remarkably plane profile with a slope which varies very little alongshore (see Figure 1 of *Guza and Thornton*, 1980].

A total of 42 sensors were deployed over an area 520 m long parallel to the shore and up to 500 m offshore. This paper deals with data from 19 two-component electromagnetic flowmeters, ten on a longshore line about half way across the surf zone, and ten on a shore-normal line going from the swash zone to well beyond the break point (Figure 2). The sensors, Marsh-McBirney 4 cm diameter probes, are described by *Guza and Thornton* [1980], who estimate that the recorded currents are accurate to about ±5%. Data from the sensors were telemetered to a shore station where they were recorded on the logging system described by *Lowe et al.* [1972]. The initial sampling rate was 64 samples/s, which was then low-pass filtered and reduced to 2 samples/s.

The two days discussed here were chosen because the incident wave conditions were simplest, the spectra being dominated by narrow swell peaks, with a period of about 15 s. An unusual feature of both days was the visual observation of very distinct long period fluctuations of surf zone width associated with a well-defined alternation of groups of high and low waves in the incident wave field. Figure 3 shows the average on/offshore flow spectrum from all the sensors in the longshore line on November 20. The sharp swell peak at about 0.07 Hz is clear, with a broader first harmonic; *Guza and Thornton* [1980] show that at least three harmonic peaks can be seen in spectra from this day. There is also an important contribution to the total energy from the surf beat band, in the period range 30–200 s. It is this energy which we investigate in this paper.

Analysis Considerations

Edge wave motion is characterized by a dispersion relation relating the longshore wave number k (= $1/L$, where L is the longshore wavelength) to the wave frequency f (= $1/T$, where T is the wave period). For shallow water waves on a beach of linear slope angle β (i.e., when $(2n + 1)\beta \ll 1$; *Guza and Davis* [1974]) the dispersion relation for small amplitude waves is given by [*Eckart*, 1951].

$$f^2 = \frac{gk}{2\pi}(2n + 1)\tan\beta \tag{1}$$

where n is any positive integer or zero, and characterizes an infinite, discrete set of edge wave modes at any given frequency or wave number. For longshore progressive waves, the corresponding offshore current u and longshore current v are given by

$$u(x,y,t) = \frac{a_n g k}{f}\frac{\partial}{\partial\chi}[L_n(2\chi)e^{-\chi}]\cos 2\pi(ky - ft) \tag{2}$$

$$v(x,y,t) = -\frac{a_n g k}{f}L_n(2\chi)e^{-\chi}\sin 2\pi(ky - ft) \tag{3}$$

$$\chi = 2\pi kx$$

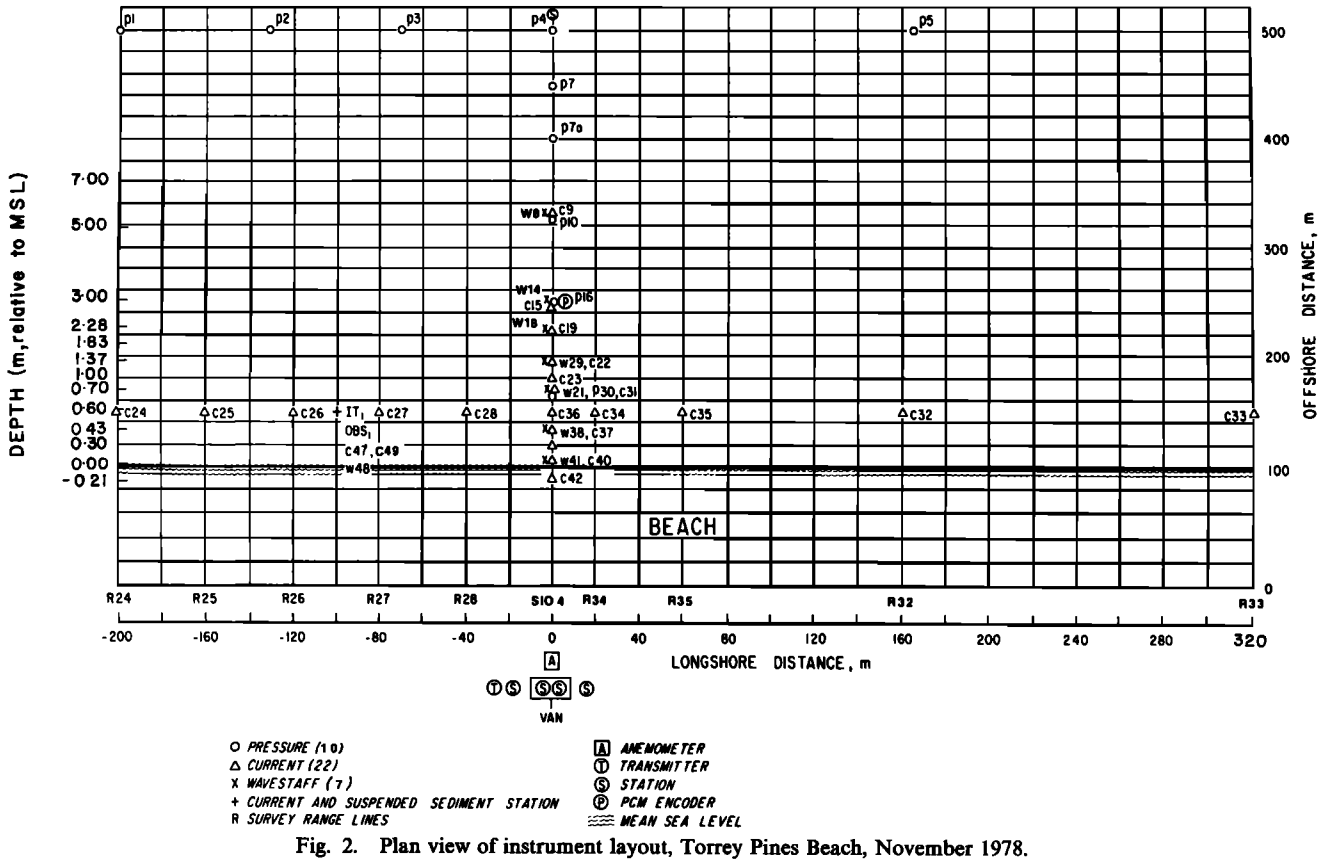

Fig. 2. Plan view of instrument layout, Torrey Pines Beach, November 1978.

where x, y are horizontal coordinates in the offshore and longshore directions, $L_n(2\chi)$ is the Laguerre polynomial of order n, and a_n is the shoreline amplitude of the mode n edge wave.

A major purpose of this investigation is to use the longshore line of current sensors to detect the longshore wavelengths of the measured velocity field and hence identify edge wave motion. If the wave field is homogeneous along the longshore array and stationary in time during the measurement period, then well-established objective procedures can be used to determine the two-dimensional energy spectrum, $S(k, f)$, which gives the energy in the wave field as a function of both frequency and wave number. In particular, if progressive edge waves are present, we should see energy lying along ridges in f, k space corresponding to a dispersion relation like (1).

Techniques for estimating the two-dimensional energy spectrum are discussed by *Munk et al.* [1964] and *Davis and Regier* [1977]. The two-dimensional spectrum of a function $u(x, t)$ is given by

$$S(k, f) = \int S^1(\eta, f) \exp(-2\pi i k\eta)\, d\eta \tag{4}$$

where

$$S^1(\eta,f) = C(\eta,f) + iQ(\eta,f) = \frac{1}{\tau}\langle F_x F_{x+\eta}{}^* \rangle \tag{5}$$

and

$$F_{x_0} = \int_{-\tau/2}^{+\tau/2} u(x_0,t) e^{-i2\pi f t}\, dt \tag{6}$$

where τ is the length of the time series. $S^1(\eta,f)$ is known as the displaced (or spatially lagged) frequency cross spectrum between two records taken from sensors separated alongshore by a distance η; C and Q are the displaced co- and quadrature spectra, respectively. *Munk et al.* [1964] show that the Fourier transform (4) of C alone gives the sum of contributions to the power spectrum from waves traveling in opposite directions parallel to the shore, while the Fourier transform of Q alone gives the difference in energy between the waves traveling in opposite directions. The angle brackets in (5) indicate that some form of averaging of the F product, in frequency space or time, is done to obtain statistically stable estimates of the displaced cross spectra.

The analysis therefore consists of three steps. First, the fast Fourier transform technique is used to obtain the Fourier amplitudes F for each sensor in the longshore array (6). These are then multiplied together and averaged appropriately to form a matrix of values of $S^1(\eta,f)$ (5). Finally, $S^1(\eta,f)$ is transformed to give the 2-D spectrum $S(k,f)$ (4).

In order to resolve in (k,f) space the dispersion curves of (1), care must be taken in choosing bandwidths of the spectrum estimates both in wave number and in frequency. Generally in computing directional spectra the frequency bandwidth can be made very small by taking a long enough record. In the present case, however, the total record length was limited by the need to use data for which the mean water level was essentially steady. A change in level of 20 cms on this beach produces about a 10 m horizontal change of the shoreline position, and, since the offshore profile of edge waves scales as $kx \sim f^2 x$ (equations (1)–(3)), this shoreline change is equivalent to a ~10% change in frequency at the longshore array. By recording over the time of high tide, approximately 3-hour long records were obtained for which the mean level

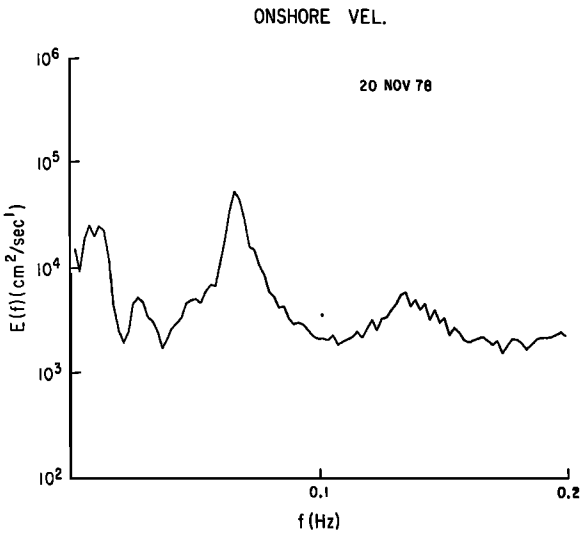

Fig. 3. Average spectrum of on/offshore velocities measured by the nine sensors (excluding C26) in the longshore line, November 20, 1978.

change was less than 20 cms. Blocks of 4096 data points (2048 s), were Fourier analyzed and the cross spectra found from them were averaged over five blocks to obtain estimates with a frequency bandwidth of 4.9×10^{-4} Hz and 10 degrees of freedom. Despite the rather small number of degrees of freedom associated with these estimates, the bandwidth of 4.9×10^{-4} Hz was chosen so that the equivalent wave number resolution for edge waves, related to the frequency bandwidth through the dispersion relation (1), was sufficiently small to allow separation of mode 0 and mode 1 waves even at the low frequency end ($\sim 5 \times 10^{-3}$ Hz) of the surf beat band.

As a detector of the longshore wavelengths of long period edge waves the longshore sensor array is clearly not ideal (the array configuration was chosen with other purposes primarily in mind). A simple Fourier transform of the displacement cross spectrum, of the form shown in (4), would result in a resolution in k space of only $1/520 = 1.9 \times 10^{-3}$ m^{-1}. With this resolution, edge waves of modes 0 and 1 would only be resolved at frequencies greater than about 0.013 Hz, modes 1 and 2 at 0.03 Hz and so on. Fortunately, the maximum likelihood method (MLE), described in detail by *Davis and Regier* [1977], provides a much finer resolution and is particularly well suited to resolving the sharp peaks expected for the discrete edge wave modes. The MLE technique was therefore used here.

Longshore Currents

For reasons which will become apparent, we consider first the longshore currents alone. The average offshore distance of the sensors in the longshore line on both of these days was 53.5 m, but this varied along the array, with a standard deviation of about 4 m. In order to allow for the slight differences in signal amplitude resulting from these differences in offshore position (and possibly from small errors in sensor calibration) each calculated cross-spectral estimate was normalized by the square root of the product of the two measurements of energy provided by the sensor pair. Figures 4*a* and 4*b* show the normalized displaced cospectra for a range of frequencies on the two days investigated. The scatter of points, due at least in part to the statistical uncertainty of each estimate, is evident, but the redundancy of the array in contributing several estimates at many of the separation distances to some extent compensates for this scatter. A clear trend in the shape of the displaced cospectra with frequency can be discerned on both days; the wavelength of a smooth curve drawn through the points would decrease with increasing frequency. The heavy stars in Figures 4*a* and 4*b* indicate the predicted zero crossings of the displaced cospectra for a mode 0 edge wave on a beach of slope 0.02; the observations appear to be in very good agreement with these predictions. The figures also make clear the limitations of the array for detecting edge wave wavelengths. The maximum longshore displacement is comparable with predicted longshore wavelengths. The rate of change of zero-crossing position with frequency also shows that further frequency smoothing to reduce the scatter on the cospectral estimates would significantly smear the trends of the displaced cospectra. In contrast to the cospectra, the quadrature spectra on these days showed no clear shape, with points apparently scattered about zero for all displacements.

Transformation of the full array of displaced cospectra, using the MLE technique, results in the two-dimensional spectra shown in Figures 5*a* and 5*b*. The contours show the 'enhancement factor,' which is the ratio of the observed energy to the energy which would occur if the total energy at each frequency were evenly smeared over k space to wave number limits of ± 0.025 m^{-1}. (Since the array did not provide longshore separations at all multiples of the smallest separation (20 m) up to 520 m, these wave number limits may be slightly above the Nyquist wave numbers of the array. However, the spectra shown in Figures 5*a* and 5*b* suggest that aliasing is not a problem with these data.) Energy levels at surf beat frequencies were very similar on the two days, as can be seen (for on/offshore currents) in Figures 3 and 7. A number of interesting conclusions can be drawn from these two-dimensional spectra.

Energy is clearly clustered around ridges in (f,k) space on both days, as we expect for free wave motion obeying a well-defined dispersion relation. Figure 6 shows a detail of Figure 5*b*, emphasizing this clustering, and also showing the essential symmetry of the energy spectrum for November 21, implying that the observed low frequency energy was about equally divided between waves propagating northward and southward along the array.

Two predicted dispersion curves are shown in Figure 5*a* to compare with the observations. The broken lines are the dispersion curves calculated by the Runge-Kutta technique described by *Holman and Bowen* [1979], using the measured offshore profile for the center line of the array. As expected, these curves differ little from predictions for a beach of linear slope, the equivalent beach slope being $\beta = 0.0194 \pm 0.0011$ over the frequency range 0.003–0.030 Hz. The solid lines show the predicted dispersion curves for a beach of linear slope $\beta = 0.023$ (equation (1)). Despite the uncertainty in defining the locus of the observed energy maxima, there are strong indications on both days, and for both modes 0 and 1, that the predictions based on the larger beach slope are in better agreement with the observations at all frequencies.

There are several factors which might be contributing to an apparent increase in the beach slope for these dispersion curves. First, the edge waves may be sufficiently strongly damped by viscosity to experience changes in the dispersion relation. *Mei and Liu* [1973] have shown that if there is an

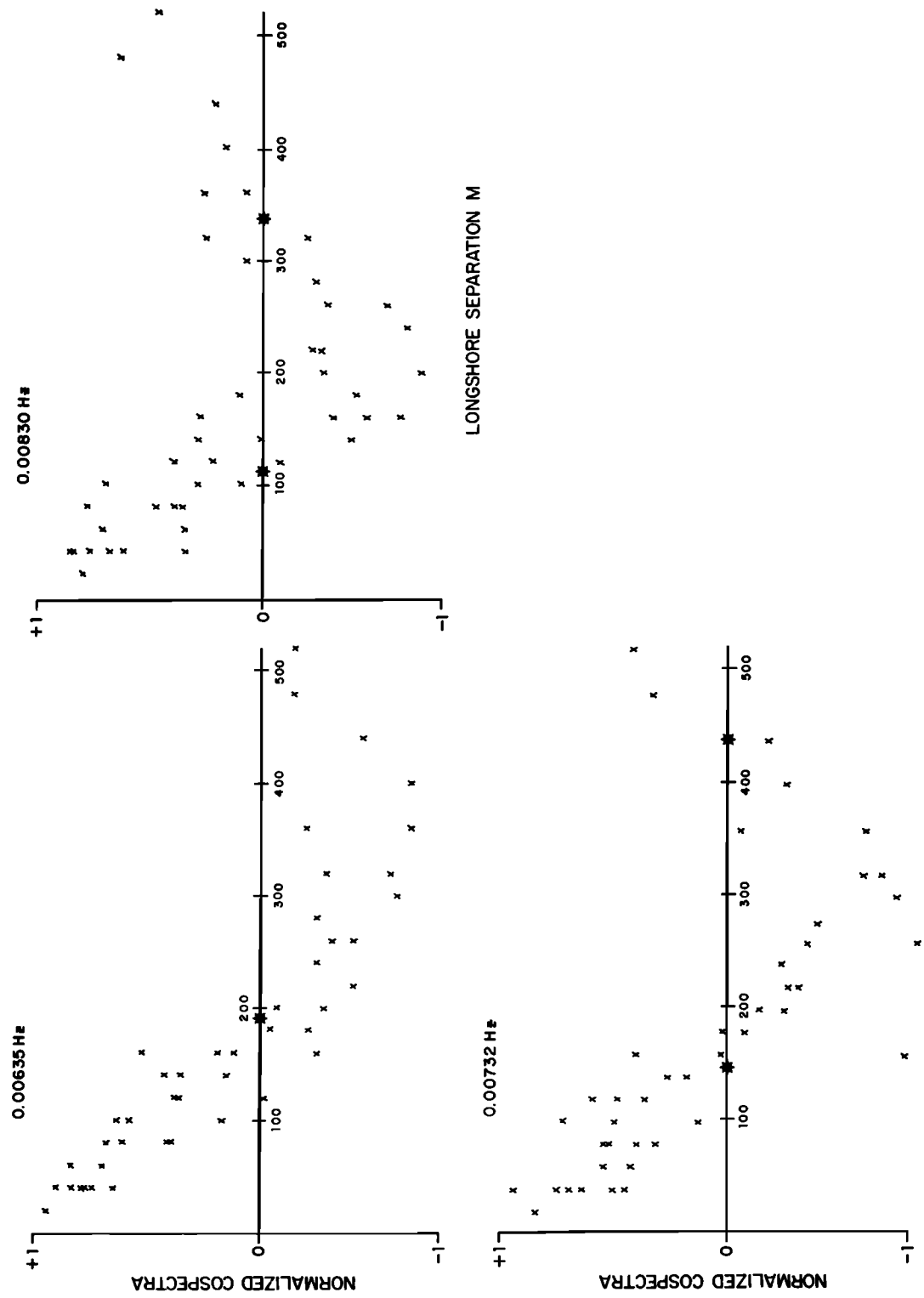

Fig. 4. Normalized cospectra of longshore current as a function of sensor separation. The heavy stars indicate the separations at which zero crossings are predicted for a zero mode edge wave on a beach of slope 0.02. The frequencies shown are in the high energy surf beat band and, for clarity, only alternate frequency estimates are shown. (*a*) November 20, 1978. (*b*) November 21, 1978.

Fig. 4*a*

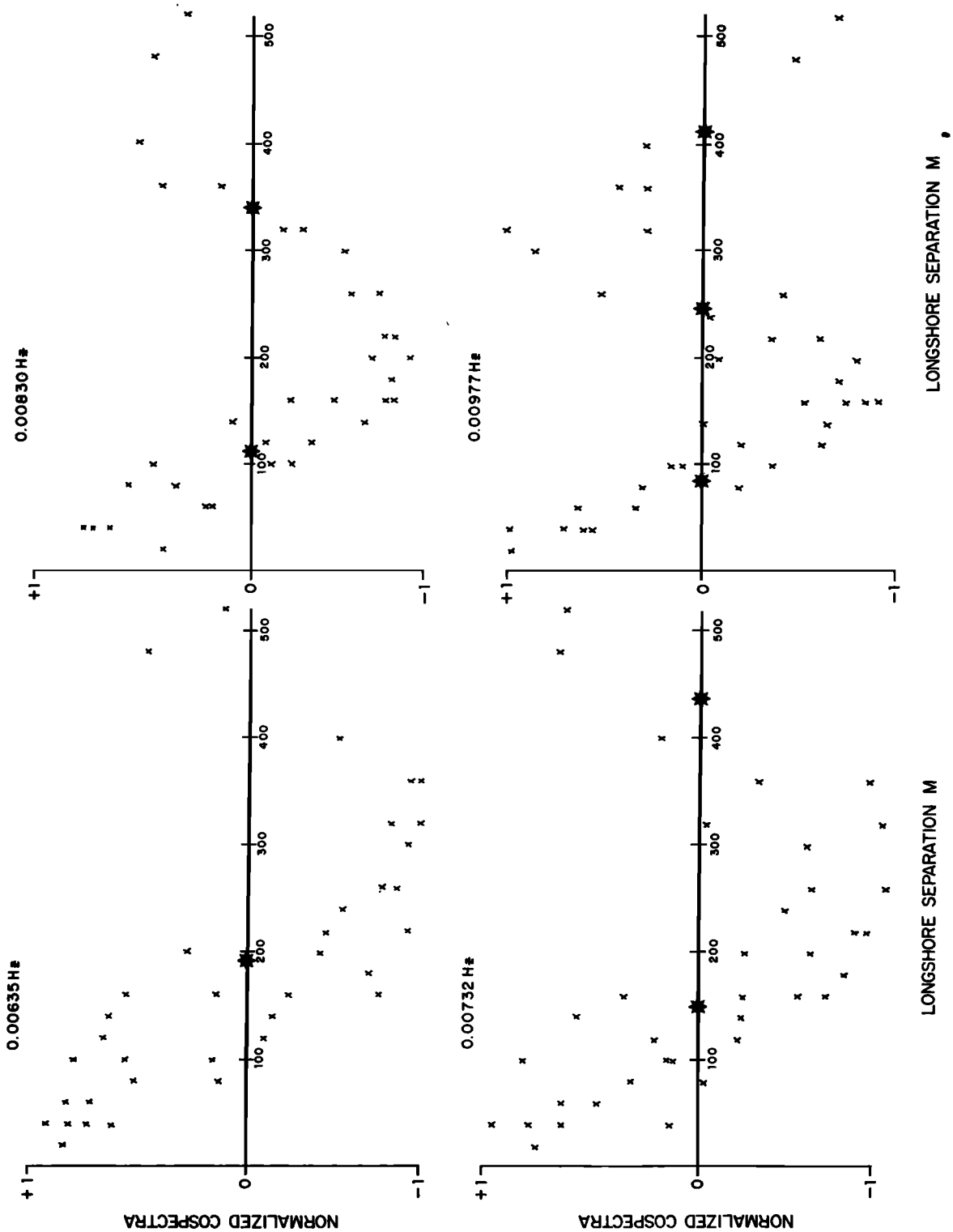
0.00830 Hz
0.00977 Hz
0.00635 Hz
0.00732 Hz
NORMALIZED COSPECTRA
LONGSHORE SEPARATION M
+1
0
-1
100
200
300
400
500

Fig. 4b

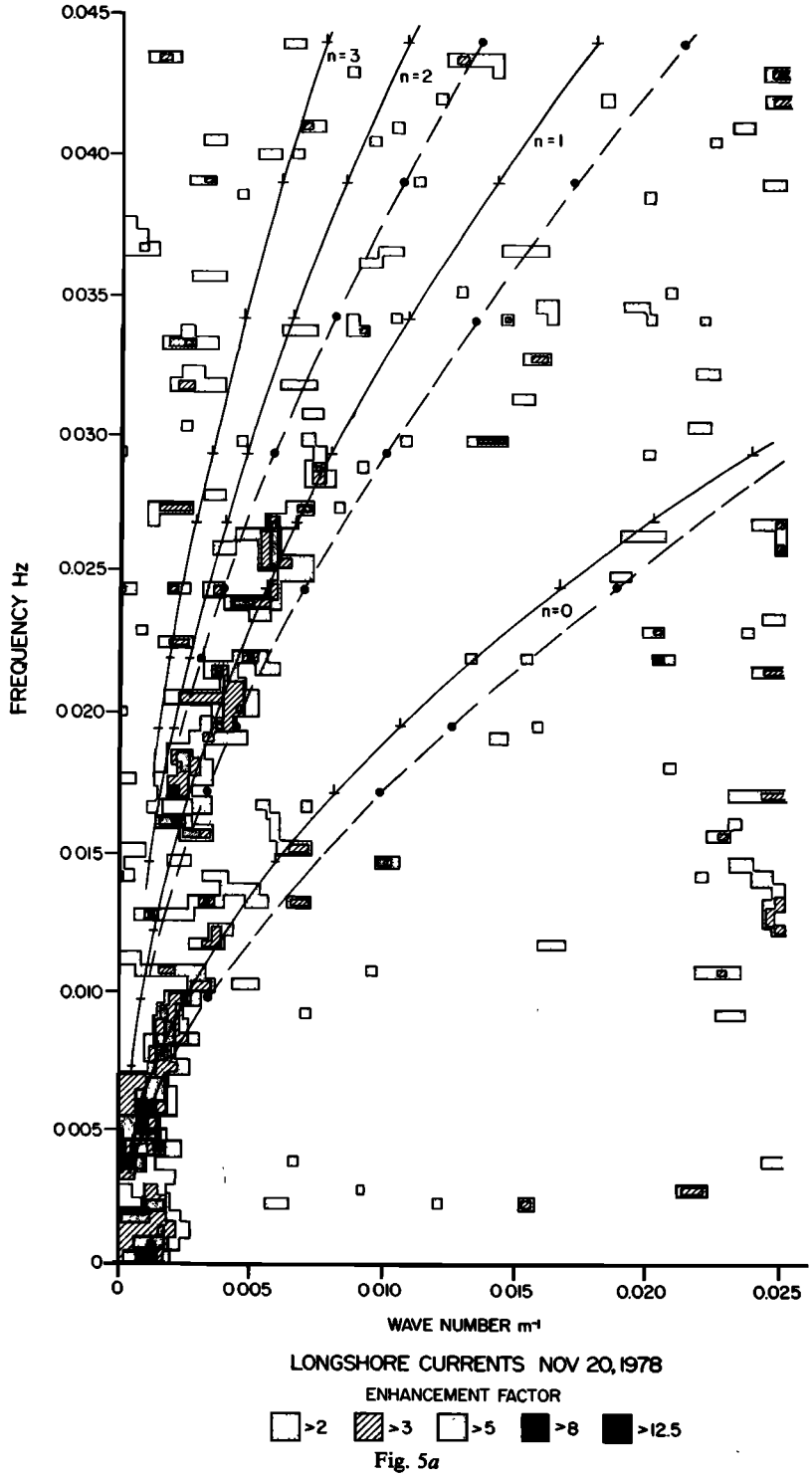

Fig. 5*a*

Fig. 5. Two-dimensional spectra of longshore current energy. Shown is the average energy propagating northward and southward along the shore. Contours give the 'enhancement factor,' defined as the ratio of the observed energy to the energy which would be observed if the energy at a given frequency were uniformly distributed across k space to an upper wave number of 0.025 m^{-1}. The solid lines give the predicted dispersion curves for the first five edge wave modes on a plane beach of slope $\beta = 0.023$. (*a*) November 20, 1978. The dashed line shows the dispersion curves for the measured beach profile, calculated using a Runge-Kutta technique. (*b*) November 21, 1978.

imaginary frequency component associated with viscous damping, then there is a change in the real frequency (for fixed wave number) of the same order. Since the edge waves span the turbulent surf zone, damping is likely to be stronger than that associated with laminar boundary layers, but a quantitative calculation is not possible at present. Second, monochromatic progressive edge waves are known to have a finite amplitude term in their dispersion relation [*Guza and Bowen*, 1976] similar to that for deep water Stokes waves. The effect of this finite amplitude term is to decrease k at any fixed frequency and thus is equivalent to an apparent increase in beach slope. However, while this trend is in agreement with

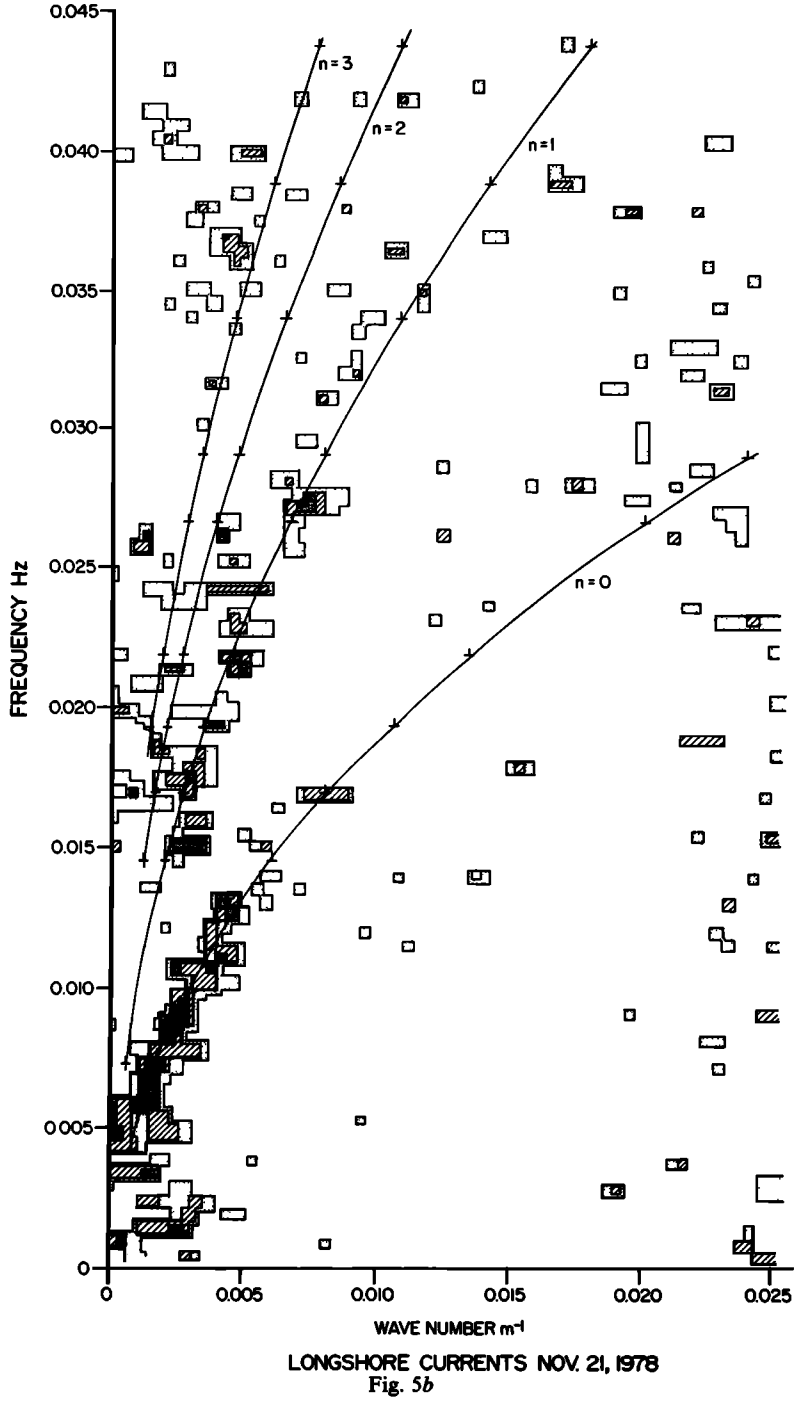

Fig. 5*b*

our observations, the quantitative monochromatic results are not directly applicable to the much more complex conditions of a continuum of progressive edge waves nonlinearly coupled to incident wave groups. Third, while the measured beach slope remained essentially constant over a longshore distance roughly equal to a typical edge wave wavelength, and no major changes occurred for at least 2 km on either side of the study site (Figure 1), a 15% change in mean beach slope over some appropriate longshore averaging scale is certainly plausible. Considering these sources of uncertainty, it is perhaps surprising that the observed dispersion curves are as close to the predicted curves as they are. In the discussion to follow, a beach slope of 0.023 has been chosen in all calculations involving the longshore array.

Separation of Modes

A prominent feature of the observed dispersion ridges in Figures 5*a* and 5*b* is the apparent domination of one single mode, either mode 0 or mode 1, throughout the low frequency band. This is most clearly shown in Figure 5*b*, where mode 0 dominates from about 0.005 Hz to 0.014 Hz and mode 1 above 0.014 Hz. Neither figure shows evidence for edge wave energy above mode 1. The lack of obvious mode 1 energy below 0.014 Hz is emphasised by the higher resolution plot of Figure 6. Although background energy levels are somewhat higher on the low wave number side of the $n = 0$ ridge than on the high wave number side, there is no evidence for energy peaks either along higher modes lines or at zero wave number.

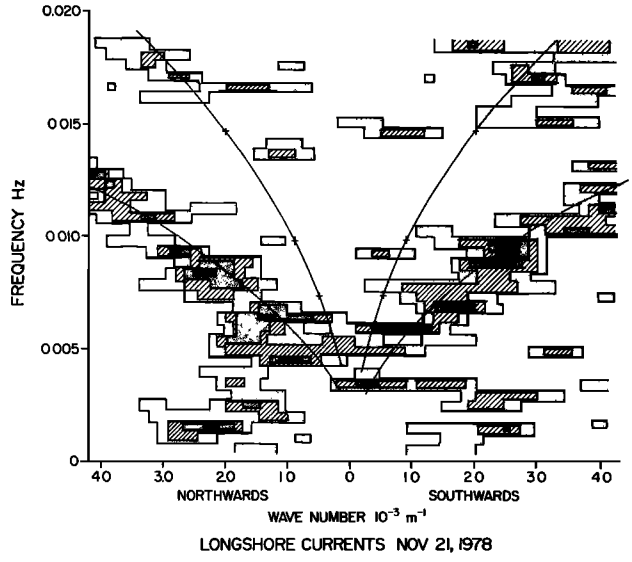

Fig. 6. Part of the two-dimensional longshore current spectrum for November 21, 1978, showing the separation of energy propagating southward and northward along the shore. Predicted curves are for $n = 0$ and $n = 1$ assuming a plane beach of slope $\beta = 0.023$. The contour shades are the same as for Figure 5*a*.

The apparent separation of modes into different frequency bands is in part due to the existence of nodes in the offshore profile of edge waves at particular frequencies. The Laguerre function terms in (2) and (3) have n zero crossings in the offshore profiles, where n is the edge wave mode number. These zero crossings occur at certain values, χ_n, of the dimensionless offshore length scale parameter $\chi = (2\pi f)^2 x/g \tan \beta$. Furthermore, the mth zero crossing position χ_m varies very little with mode number for mode numbers $n \geq m$ [see, e.g., *Guza and Inman,* 1975, Figure 1]. Hence for a sensor at a given offshore location, there are a series of frequencies for which all edge wave modes are either close to a zero crossing or are in their exponentially decaying tails. The zero crossings for waves incident from arbitrary angles of incidence and reflected at the shoreline also essentially coincide with the zero crossings of edge waves of the same frequency [*Guza and Bowen,* 1975]. Thus any combination of edge wave modes and totally reflected incident waves will produce, at a given current meter, velocity spectra with minima at predictable frequencies. Of course, since all sensors in the longshore line are at essentially the same offshore distance, they all show minima at the same frequencies.

Figure 7 shows the low frequency portions of spectra of u and v measured by one of the sensors in the longshore line, where $x = 58$ m. The vertical arrows show the predicted frequencies of zero crossings for modes 1 and 2 and for $n \to \infty$ (corresponding to an almost normally incident reflected wave) for a beach slope $\tan \beta = 0.023$. The predicted and observed frequencies for spectral minima are in very good agreement, with the low mode number predictions in somewhat better agreement than the assympototic values.

The first mode zero crossing for v occurs at $f = 0.0125$ Hz, and it is reasonable to assume that we must be about ± 0.0015 Hz away from the zero-crossing frequency in order to observe edge wave energy, since mode 1 energy begins to appear at 0.014 (Figure 5). Based on this, we cannot be certain that mode 1 or higher mode energy does not exist in the band $0.011 \to 0.014$ Hz, and it may be coexistent with mode 0 in this range. Below 0.011 Hz, however, longshore currents are not near a node for any edge wave mode. The observations therefore imply that only mode zero is present at least for $f <$ 0.011 Hz. There may also be a hint of a minimum corresponding to $n = 2$ and higher modes at about 0.03 Hz in the longshore spectrum of Figure 7, but this is higher than the frequencies for which dispersion ridges are observed in Figure 5*a*, and the minimum is therefore poorly resolved.

We note in passing that predicted and observed frequencies for spectral minima are also in good agreement for on/offshore velocities (Figure 7). The first and second minima are clear, with possibly even a third minimum. The lowest frequency ($\simeq$0.005 Hz) minimum is not associated with nodes in the on/offshore wave profile and may be due to a roll-off in edge wave forcing, as we shall see later. Cross-spectral analysis between sensors in the on/offshore line shows that energy above about 0.05 Hz is associated with progressive incident waves. Spectral minima for on/offshore velocity measured at different offshore distances, using sensors in the shore-normal line, change frequency in a manner completely consistent with the predicted zero-crossing frequencies, as would be expected from *Suhayda* [1974] and *Huntley* [1976]. Several authors [*Wright et al.,* 1979; *Sasaki and Horikawa,* 1979; and others] have interpreted some apparent spectral peaks as evidence for the preferential excitation of certain surf beat frequencies, rather than as being due to the existence of nodes in the on/offshore profiles [see also *Huntley,* 1980*b*]. In fact, as predicted by (2) and (3), observed minima in longshore velocity occur at essentially the same frequencies as maxima in on/offshore velocity and vice versa (Figure 7). This is further evidence for a broad band of surf beat energy with no preferentially excited frequency bands.

The reasons for frequency separation of edge wave modes are not clear. One possibility, discussed by *Bowen and Guza* [1978] and *Holman* [1979] is that it is a result of the forcing of edge waves by narrow frequency band incident waves. *Bowen and Guza* [1978], following *Gallagher* [1971], show that two monochromatic incident waves of frequency f_1 and f_2 and deep water angles of incidence α_1 and α_2 can interact to form edge waves at the difference frequency

$$f_e = f_1 - f_2 \qquad f_1 > f_2 \tag{7a}$$

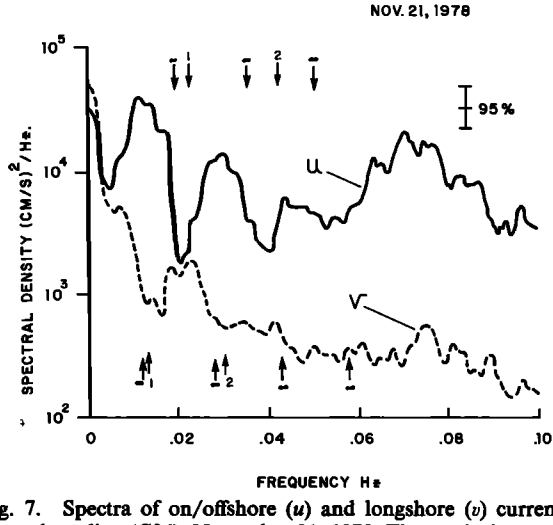

Fig. 7. Spectra of on/offshore (u) and longshore (v) currents at the longshore line (C24), November 21, 1978. The vertical arrows indicate the predicated locations of nodes in u (upper arrows) and v (lower arrows) for edge waves of mode 1, 2, or ∞.

if

$$f_e^2 = |f_1^2 \sin \alpha_1 - f_2^2 \sin \alpha_2| \sin (2n + 1)\beta \qquad (7b)$$

If the incident waves approach from the same deep water direction α, these conditions reduce to

$$f_e = 2f_0 \sin \alpha \sin (2n + 1)\beta \qquad (8)$$

where $2f_0 = f_1 + f_2$. For a narrow incident wave spectrum, (8) predicts a series of discrete edge wave peaks, each corresponding to a different mode number, with the peaks smeared out in frequency by the directional spread or frequency spread of the incident waves.

For the data shown in Figures 5*a* and 5*b*, (8) cannot apply since the edge wave frequencies are too high relative to incident wave frequencies (sin α is found to be greater than 1). Thus colinear incident waves cannot cause the observed frequency separation. However, swell waves approaching Torrey Pines Beach are partially shadowed by the offshore islands of San Clemente and Santa Catalina, and by La Jolla Point to the south, and this results in distinctly bimodal directional spectra for the incident swell (S. Pawka, private communication, 1980). Thus, for example, the directional spectrum for November 20, estimated (by maximum likelihood methods) using the longshore line of pressure sensors (*P*1–*P*5, Figure 2), shows that at 10 m depth the incident swell waves approached the beach with distinct directional peaks at about 2°S and 6°N relative to the shore normal. Assuming that Snell's law is appropriate for describing the refraction of these waves, the equivalent deep-water angles of approach are 5 ± 2°S and 20 ± 3°N, in good agreement with expected swell windows around San Clemente Island. Using these incident angles, and assuming that interaction takes place between frequencies symmetrically placed about the swell peak frequency (= 0.067 Hz), equations (7*a*) and (7*b*) predict edge wave frequencies of $(6.7 \pm 0.7) \times 10^{-3}$ Hz and $(11.6 \pm 1.6) \times 10^{-3}$ Hz, respectively, for modes 0 and 1. Whilst these values are perhaps somewhat lower than one would estimate from Figure 5, the agreement with observations is not unreasonable in view of the uncertainties inherent in the predictions (particularly in estimating the offshore directional spectra); as discussed above, any mode one energy between 0.011 and 0.014 Hz would be suppressed because of the nodal structure.

There is one aspect of the observations that appears to be at variance with this otherwise consistent explanation. Equations (7*a*), (7*b*), and (8) can be used to estimate the bandwidths of the peaks at each mode number due to angular spread about the mean angles α_1 and α_2. On this basis, the observed bandwidth of the zero mode (Figure 5) is significantly larger than predicted. In fact $\alpha_1 (= -\alpha_2)$ must approach 90° in order to spread zero mode energy up to 0.014 Hz. Interaction between incident waves with frequencies above the main swell peak would not require so large an angle and may therefore provide an explanation for this energy.

It is possible that some other constraint prevents, or at least discourages, the coexistence of more than one mode at any given frequency. The laboratory experiments of *Bowen and Inman* [1969] and *Guza and Inman* [1975] for reflective beaches certainly suggest that a single mode generally dominates the nearshore flow field with other modes, if present at all, being much smaller. For the special case of synchronous edge waves (those with the same period as the incident waves), *Bowen and Inman* [1969] found a transition between $n = 0$ dominance and $n = 1$ dominance which occurred at a particular value of the nondimensional surf zone width $(2\pi f)^2 x_b/g \tan \beta$, although there was some overlap between the modes. The nondimensional surf zone width represents a ratio between the length scales of the surf zone and of the offshore decay of edge waves, and it has been suggested [see, e.g., *Guza and Bowen*, 1977] that the ratio is important because edge waves with a significant fraction of their energy within the surf zone may be not only strongly damped by the increased eddy viscosity there due to wave breaking but also only weakly forced by the wave groups which occur principally outside the surf zone [see also *Holman*, 1979]. For both of the days considered here the surf zone width was about 100 m, and if we assume a transition frequency of 0.014 Hz separating regions of $n = 0$ and $n = 1$ dominance the dimensionless surf zone width for the transition becomes 3.4. Intriguingly this value is not significantly different from the value of between 2.00 and 2.85 found for synchronous waves by *Bowen and Inman* [1969]; taking the transition frequency as 0.012 Hz, which is clearly possible in view of the masking effect of the zero crossing in Figure 5, leads to a dimensionless surf zone width of 2.5.

Distribution of Longshore Current Energy

If we take a wave number bandwidth of 1.25×10^{-3} m^{-1} around the edge wave dispersion line for $\beta = 0.023$ for November 21 (Figure 5*b*), the percentage of the total energy in this band for $n = 0$ is 30% ± 15% at each frequency in the range 0.006–0.013 Hz, and has the same range of values for the $n = 1$ band for frequencies in the range 0.0145–0.023 Hz, with the percentage falling off at frequencies above this. Similar percentages are found for November 20 (Figure 5*a*) though there is a greater scatter of values. The remaining energy is broadly scattered thoughout the wave number space, with apparently random peaks sometimes occurring right out to the Nyquist wave number. There is some evidence that this background energy is 'pink,' but the increase in energy toward zero wave numbers is relatively weak. Thus for both days the average enhancement factor (energy observed/energy assuming white spectrum in k) is only 1.9 at wave numbers below the $n = 0$ band in the frequency range 0.007–0.012 Hz, and below $n = 1$ band in the frequency range 0.015–0.020 Hz. There is no evidence that this enhancement is greatest at zero wave number.

As discussed in the introduction, there are a number of possible sources of energy which will not lie on the edge wave dispersion curve. One possible source is forced wave motion, the nonresonant driving of longshore and on/offshore currents by incident wave groups with a broad range of incident wave numbers. Other analysis of this data has shown that such forced wave motion does indeed exist, at least in the on/offshore velocity field (R. T. Guza and E. B. Thornton, manuscript in preparation, 1981). However, for an incident wave spectrum which is narrow in both frequency and angular spread the range of wave numbers forced by nonlinear interaction will be small and centered at a low wave number. Equation (8) will also apply to forced wave wave numbers and, as for the edge waves, forced waves are unlikely to occur with wave numbers much above 2×10^{-3} m^{-1} if interaction between waves in the main swell peak is responsible for generating the forced motion. Thus forced waves probably can only contribute to the slight rise in energy at low wave number and not to the broad spread out to large wave numbers.

Of the possible sources of additional free wave energy, the

leaky modes would occupy only a small fraction of (f, k) space near $K = 0$. The line separating trapped and leaky modes in (f, k) space (the 'cut-off' line) is the dispersion line for free waves propagating parallel to the shore at $x = \infty$. *Munk et al.* [1964] calculated the cut-off line for the region of the southern California continental shelf, assuming that the appropriate waves at $x = \infty$ were shallow water waves on the plateau of the continental shelf at a depth of about 1 km. In this case the cut-off line is a straight line with a slope of 98 m/s. For most of the low frequencies studied here, however, the shallow water criterion does not apply for a depth of 1 km. Above 0.025 Hz the deep water cut-off criterion of Ursell is appropriate and, for a linear beach slope of 0.023, the cut-off line corresponds approximately to the dispersion line for a mode 34 edge wave. Using a depth of 1 km for the lower frequencies, the calculated cut-off line goes through 4.0×10^{-4} m^{-1} at $f = 0.025$ Hz and 9.5×10^{-4} m^{-1} at $f = 0.045$ Hz. There is no evidence for enhanced energy within this narrow region of (f, k) space.

There is some evidence for standing edge waves in the on/offshore current data, as we shall see later. These waves should also appear in the longshore currents, although their energy levels may be lower, at least for modes above zero. The appearance in (f, k) space of waves with a standing wave pattern alongshore is hard to assess, since it will depend critically on the location of nodes and antinodes relative to the sensor array. In the displaced cross spectra the results for the same separation but different absolute position along the array will differ, and this would contribute to the scatter in these diagrams. Thus it is possible that spreading of energy through k space is a result of some standing edge wave energy along the array. The results for on/offshore currents (see below) suggest, however, that the energy is still confined within a region bounded at high wave number by the progressive edge wave dispersion curves.

We are thus lead to the conclusion that, other than some low wave number enhancement, most of the spread of longshore current energy to higher wave numbers is due to inadequacy of the analysis techniques. The most obvious source of this is the scatter seen on the displaced cospectrum plots in Figure 4. Interestingly, despite the obvious limitations of the spatial layout of the array, this scatter is due to inadequate sampling in time rather than in space. If statistical uncertainty is the main source of the energy spread, then the (30 ± 15%) of the total energy found around the dispersion curves must be considered a lower limit on the percentage of longshore current energy contained in progressive edge waves on this beach.

OFFSHORE PROFILES

The 10 flow sensors along a line perpendicular to the shoreline can be used to look at the offshore profile of the edge waves found using the longshore array. Figure 8 shows two representative results. Figure 8*a* shows results at $f = 0.00781$ Hz, within the $n = 0$ edge wave band, and Figure 8*b* shows results at $f = 0.01563$ Hz, within the $n = 1$ band. The predicted curves in Figures 8*a* and 8*b* are appropriate to a beach slope of 0.020, rather than the 0.023 slope used for the two-dimensional spectra, since the resulting predictions are in somewhat better agreement with the observations. This may reflect the fact that the offshore profile responds to the local beach slope, which was close to 0.02 along the shore-normal sensor line, whilst the longshore array provides a dispersion relation for the average beach slope along the array, as discussed earlier.

The longshore currents at 0.00781 Hz are clearly consistent with the exponential offshore profile predicted for zero mode waves on a beach of constant slope. Longshore currents at 0.01563 Hz fit the predicted offshore profile for $n = 1$ rather less well, but nevertheless do show a dip in amplitude associated with the predicted zero crossing.

Cross spectra between sensors along the on/offshore line also support the predicted offshore profiles, although the values are statistically somewhat unstable at this degree of frequency resolution (Table 1). At 0.00781 Hz the phases associated with significant (at the 80% level) coherence are generally small, implying that there are no zero crossings along the array. Interestingly the low coherences observed for longshore currents occur mainly between sensor pairs straddling the breaker line, and this suggests that other processes, perhaps associated with forced waves uncorrelated with the edge waves, are occurring outside the surf zone. The large phases (with low coherence) generally associated with sensor 9 for longshore currents may be due to the presence of some mode 1 edge wave enrgy, with a zero crossing predicted to be about 140 m offshore; as we have seen, there is no evidence for progressive edge waves at this frequency (Figure 6) but longshore standing waves may be present (see next section). At 0.01563 Hz longshore current coherences are generally small when associated with sensors 37 and 39, as might be expected from the close proximity of these sensors to the predicted zero crossings (Figure 8*b*). Other phases generally confirm that a zero crossing occurs for longshore currents near sensor 37, with no additional zero crossing, which would be associated with mode 2, between sensors 15 and 9. The phase across the zero crossing is somewhat lower than the predicted 180° and may be caused by the presence of some zero mode energy overlapping into the predominantly mode 1 frequency band.

Thus the amplitudes and phases of the longshore currents measured by the on/offshore array are in reasonable agreement with predicted offshore profiles of edge wave enrgy. The offshore flows, however, are clearly not only due to the edge wave motion deduced from the longshore currents. Progressive zero mode edge waves should have an offshore flow equal to the longshore flow for all offshore distances; the observed offshore flows at $f = 0.0781$ Hz (Figure 8*a*) are substantially larger than this prediction. In Figure 8*b* the heavy dashed line in the upper graph shows the offshore currents for an $n = 1$ progressive wave predicted from the fit to the longshore currents and again there is substantially more energy than predicted in the offshore flows. The finer dashed line in this graph is an arbitrarily scaled plot of the offshore profile of a normally incident reflected free wave, or an edge wave of high mode number; forced waves propagating on- and offshore would probably also produce the same profile on average. The relative scale of offshore velocities on either side of the zero crossing seem more in agreement with this profile.

ON/OFFSHORE CURRENTS

The data discussed in the previous section suggest that, while the on/offshore currents are not inconsistent with the presence of the progressive edge waves deduced from the longshore currents, there are clearly some other sources of low frequency energy which contribute particularly to the on/offshore flow.

The two-dimensional spectrum of on/offshore flows along the longshore array (Figure 9) confirms this. In contrast to the

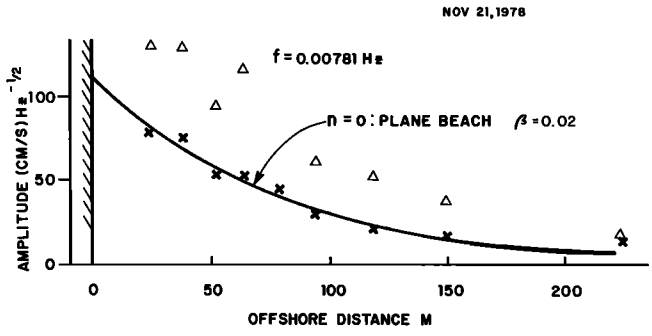

Fig. 8*a*. November 21 velocity amplitudes at 0.00781 Hz as functions of offshore distance. Crosses represent longshore currents and triangles on/offshore currents. The solid curve shows the predicted offshore profile of a zero mode edge wave on a beach of linear slope 0.02, with amplitude scaled for a best fit to the longshore currents.

longshore flow spectra in Figure 5, Figure 9 shows that energy is clustered around the zero wave number axis, with the progressive edge wave curves for modes 0 and 1 appearing to form upper bounds to the wave number spread.

There seem to be three possible explanations for these observations. First, the magnitude of longshore currents relative to on/offshore currents decreases with increasing mode number, with the shoreline amplitudes having the ratio $u/v = (2n + 1)$ for a linear beach profile. Higher mode waves therefore contribute more energy to the on/offshore flows than to the longshore flows at most offshore distances. The low wave number energy in Figure 9 may therefore be due to unresolved higher modes which are of too small an amplitude to be seen in the longshore current spectra of Figure 5. The total lack of any higher mode ridges in the longshore currents, particularly in Figure 6, seems to argue against this possibility for low modes, but higher modes could still be too small to detect from their longshore currents.

There is some rather subjective evidence that standing edge waves may be contributing to the on/offshore flows. The evidence is in two forms. First, plots of the amplitude of on/offshore flow as a function of position along the array tend to suggest some systematic variations; Figure 10 is a typical example. This variation is not the result of calibration errors. In fact, at least for limited frequency ranges, the location of the 'peak' in amplitude is found to move apparently systematically through the array as the frequency is changed. The second piece of evidence comes from the plots of displaced cospectra as a function of longshore separation. Figure 11 shows an example in which cospectra involving particular sensors have been joined by solid lines. In contrast to the longshore current cospectra, there are clearly systematic differences between the trends of cospectra involving different sensors. Figure 11 uses the same data as Figure 10, and it can be seen that there is some consistency between the two diagrams. A pure standing wave of the form sketched in Figure 10 would result in cospectra involving sensor 24 changing from +1 to −1 for sensor separations greater than about 40 m, while cospectra involving sensor 27 (but not sensors 24 and 25) would remain at +1 for all separations. Clearly then the presence of some standing wave component could produce cospectra like those in Figure 11.

Again, in order to explain the difference between the two-dimensional spectra for longshore flow and on/offshore flow, standing edge waves would presumably have to be of higher mode number than the prominent modes seen in Figure 5, i.e., $n > 0$ for $f < 0.014$ Hz and $n > 1$ for $f > 0.014$Hz.

There are, in fact, several features in the vicinity of Torrey Pines Beach which could act as reflectors of longshore progressive waves and hence set up standing waves at the array (Figure 1). About 2.6 km to the south, Scripps Canyon cuts into the smooth topography of the surrounding seabed, the head of the canyon coming to within about 275 m of the shoreline. Further south, about 5.2 km away, Point La Jolla presents a sudden, almost 90° change to the trend of the shoreline, though the offshore contours change direction more slowly. To the north the topography remains essentially unchanged for many kilometers except for a small subaqueous rock outcrop about 2 km from the array. Reflection from any of these features would probably be enhanced at longer wavelengths, and hence at higher mode numbers at any given frequency, and is therefore consistent with the observations. A particularly interesting possibility arises for reflection from the canyon head, however. Since the canyon head reaches only to within 275 m of the shoreline, it is reasonable to suppose that edge waves with offshore length scales small compared to this distance will not be reflected from the canyon head, while those with larger offshore length scales might be reflected. This idea can be roughly quantified using Figure 12, which shows the percentage of total edge wave energy shore-

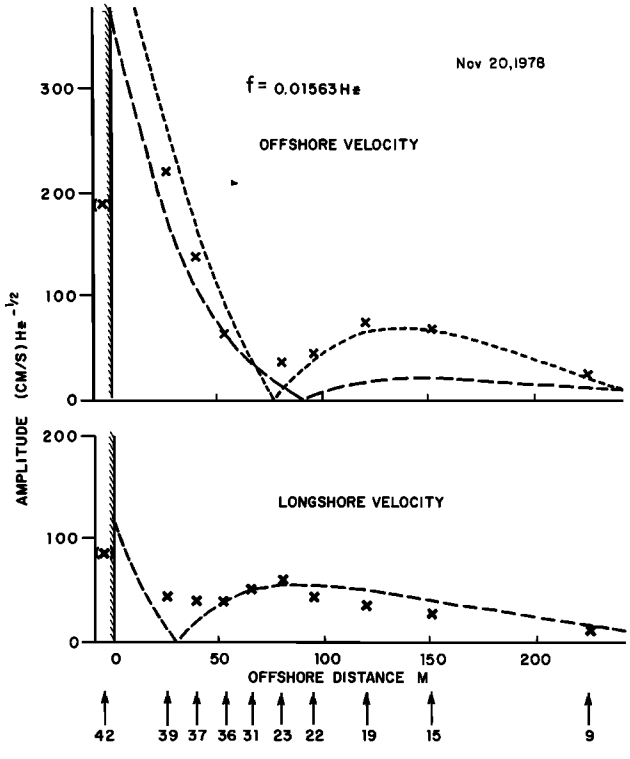

Fig. 8*b*. November 20 velocity amplitudes at 0.01563 Hz as a function of offshore distance. The crosses are data points measured by the sensors on the offshore line whose identification numbers are given by the arrows at the bottom of the diagram. The bracketed crosses were measured by sensor 42, which was only immersed for part of the time. The heavy dashed line shows the predicted offshore profiles of a mode 1 edge wave, for $\beta = 0.02$. The profile for longshore velocity has been scaled to give an approximate fit to the observations; the scale of the onshore velocity profile is then determined from the longshore velocity scale (equations (2) and (3)). The dotted line in the offshore velocity plot shows the profile for $n = \infty$ edge waves (reflected incident waves).

TABLE 1. Coherences and Phases Between Sensors Along Offshore Line

	Nov. 21: 0.00781 Hz				Nov. 20: 0.01563 Hz			
	Longshore v		On/Offshore u		Lonshore v		On/Offshore u	
Sensor Pair	Coherence	Phase	Coherence	Phase	Coherence	Phase	Coherence	Phase
42/39					[0.50	−9.0]	0.88	0.5
42/37					[0.15	168.4]	0.91	12.7
42/36					0.69	144.2	0.87	15.9
42/31					0.76	144.3		
42/23					0.82	120.4	[0.47	−95.8]
42/22					0.82	143.0	0.72	−156.8
42/19					0.89	144.8	0.93	−169.2
42/15					0.63	128.1	0.68	176.3
42/9					[0.49	101.8]	0.90	−174.5
39/37	0.89	7.0	0.99	3.7	[0.40	22.0]	0.98	8.9
39/36	0.84	−4.3	0.92	1.8	[0.08	−69.3]	0.93	9.7
39/31					[0.06	79.4]		
39/23	0.80	−1.1	0.98	1.5	[0.33	95.9]	[0.48	−54.9]
39/22	[0.47	−5.3]	0.95	−5.7	[0.29	138.6]	0.82	−157.9
39/19	[0.42	44.0]	0.94	2.5	[0.24	131.7]	0.92	−165.3
39/15	[0.28	55.1]	0.91	−1.3	[0.26	124.3]	0.93	178.3
39/9	[0.54	145.4]	0.58	29.3	[0.15	77.8]	0.92	178.2
37/36	0.97	−12.6	0.92	−3.3	0.71	−33.1	0.94	−18.2
37/31					[0.46	−45.2]		
37/23	0.82	−3.7	0.98	−2.0	[0.47	−1.8]	[0.42	−76.7]
37/22	[0.26	7.6]	0.95	−9.9	[0.52	19.7]	0.82	−165.2
37/19	[0.20	47.0]	0.96	−2.2	[0.36	−18.5]	0.93	−176.8
37/15	[0.06	−77.7]	0.93	−7.2	[0.20	−139.7]	0.87	169.7
37/9	[0.40	174.6]	[0.55	27.2]	[0.43	−70.4]	0.95	168.2
36/31					0.88	−3.4		
36/23	0.76	17.0	0.93	−1.8	0.74	−2.7	[0.35	−70.0]
36/22	[0.28	11.8]	0.83	−7.5	0.76	18.9	0.67	156.6
36/19	[0.35	53.4]	0.89	1.7	0.81	0.8	0.85	−173.4
36/15	[0.14	29.1]	0.87	−1.5	[0.51	−42.9]	0.89	173.0
36/9	[0.24	−178.2]	[0.57	18.8]	0.64	−55.8	0.95	166.0
31/23					0.70	−17.8		
31/22					0.60	5.8		
31/19					0.85	−4.4		
31/15					0.72	−47.8		
31/9					0.59	−55.8		
23/22	[0.31	15.3]	0.92	−9.3	0.94	15.9	[0.31	−100.0]
23/19	[0.31	14.3]	0.94	−1.4	0.87	14.1	[0.56	−87.8]
23/15	[0.13	−25.0]	0.88	−5.6	[0.44	3.8]	0.60	−149.0
23/9	[0.42	−172.7]	[0.52	27.0]	0.59	−55.4	[0.40	−105.1]
22/19	0.65	55.7	0.95	9.9	0.85	−1.5	0.87	−14.0
22/15	0.71	72.0	0.95	2.5	[0.47	−5.0]	0.75	−31.5
22/9	[0.51	93.8]	[0.47	27.7]	0.58	−64.8	0.68	−25.4
19/15	0.92	18.0	0.96	−8.9	0.72	−32.7	0.83	−23.9
19/9	[0.53	25.2]	[0.44	15.3]	0.77	−46.6	0.84	−13.2
15/9	0.68	3.7	[0.53	16.3]	[0.53	11.1]	0.79	−3.7

Bracketed values have coherences below the 80% confidence level of 0.58.

ward of an offshore distance x, plotted as a function of mode number and dimensionless offshore distance $\chi = \sigma^2 x/g \tan \beta$ ($\sigma = 2\pi f$). Thus if we assume, for example, that the canyon head will reflect significant edge wave energy if 50% or more of its energy lies seaward of 275 m, Figure 12 can be used to calculate 'critical' frequencies for each mode number at which this condition applies; lower frequencies than the critical will give significant reflection. Table 2 gives the predicted 'critical' frequencies for the 50% case. The prediction from this table that the minimum mode number of reflected edge waves increases with frequency agrees with the suggestion made previously, based on the difference between the longshore and offshore (f, k) spectra. In fact, Table 2 is also in reasonable quantitative agreement with Figures 5 and 9, in particular in suggesting that $n = 1$ waves become predominantly progressive above about 10^{-2} Hz, and $n = 0$ above about 0.004 Hz.

The possibility of edge wave reflection by Scripps Canyon was also suggested by *Inman et al.* [1976]. Using pressure and current sensors at the canyon, and a pressure sensor south of the canyon, they found some evidence to suggest that edge waves at discrete periods in the range 70–300 s might exist as standing waves trapped between La Jolla Point and La Jolla Canyon to the south and Scripps Canyon to the north.

Despite these encouraging indications, objective assessment of the importance of standing edge waves presents a number of problems. For example, even if the location of a reflector is assumed, it is far from clear how edge waves, with both a longshore and an offshore length scale, would reflect (if at all) from something like the canyon head. Nevertheless some objective model fitting techniques are being applied to the data in an attempt to separate the progressive and standing modes.

The third possible source of additional on/offshore energy is forced wave motion. For nearly normal incident waves the longshore length scale of wave groups will be much greater

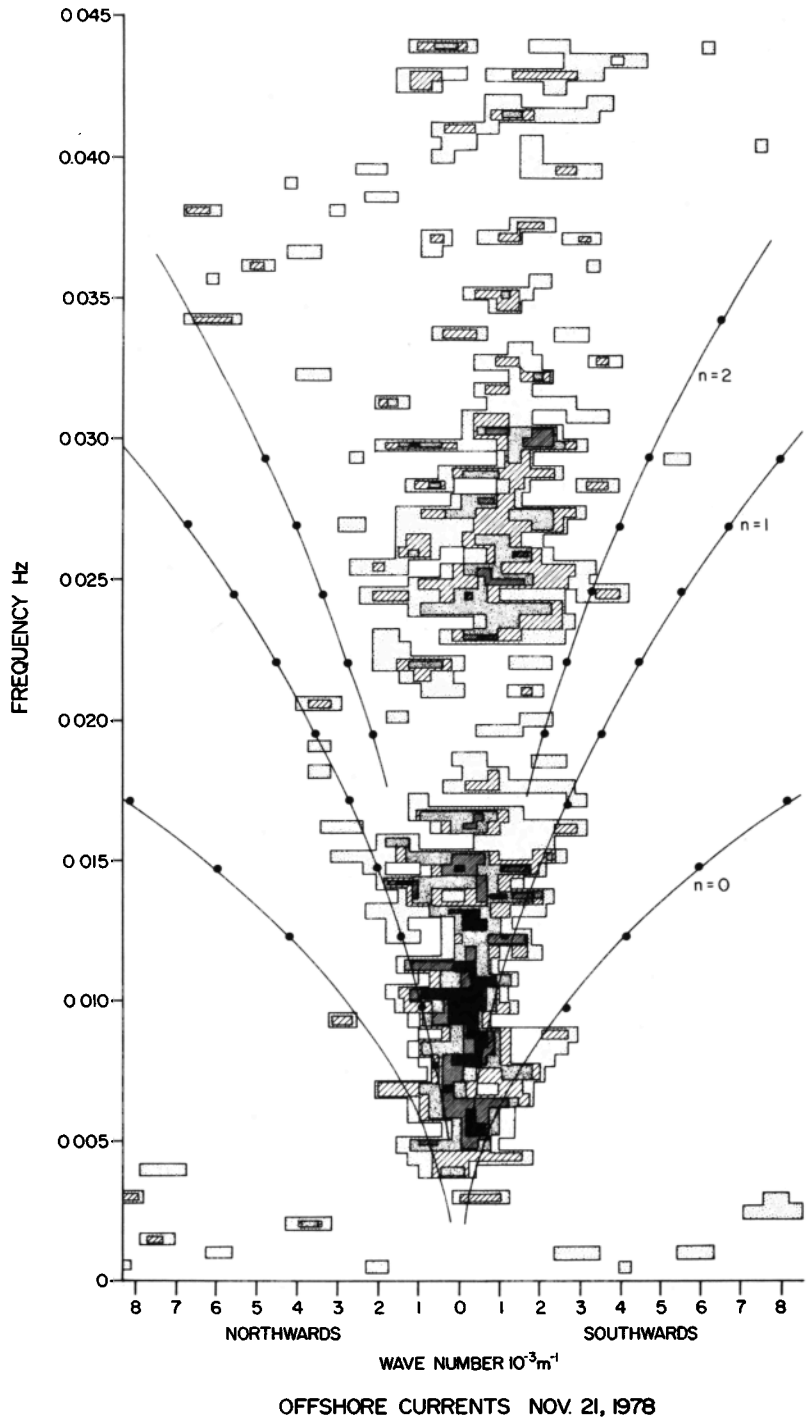

Fig. 9. Two-dimensional spectrum of on/offshore current energy, November 21, 1978. The predicted dispersion curves for the first three edge waves modes assume a beach slope of 0.023. The contour shades are the same as for Figure 5*a*.

than their offshore length scale. On/offshore forced currents may therefore be greater than longshore forced currents. Strong forced wave currents have in fact been found in the on/offshore records and their relative importance to the nearshore velocity field is being assessed (R. T. Guza and E. B. Thornton, manuscript in preparation, 1981).

CONCLUSIONS

The observations we have presented here provide the first definitive evidence that progressive edge waves are present, and have significant amplitude, in the surf-zone velocity field at surf beat frequencies. The clearest results are obtained for longshore velocities. The predicted edge wave dispersion curves, based on the measured beach profiles, are in surprisingly good agreement with the observations. There is also evidence that only one progressive edge wave mode dominates at any particular frequency, with mode zero dominating between 0.006 and 0.011 Hz, and mode one dominating between 0.014

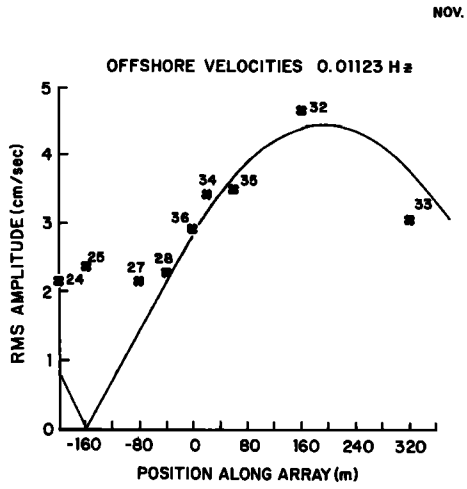

Fig. 10. Amplitude of the on/offshore current at $f = 0.01123$ Hz as a function of position along the longshore array. The solid curve sketches a mode 2 standing edge wave ($\beta = 0.023$) with a node at −160 m. Data from November 20, 1978.

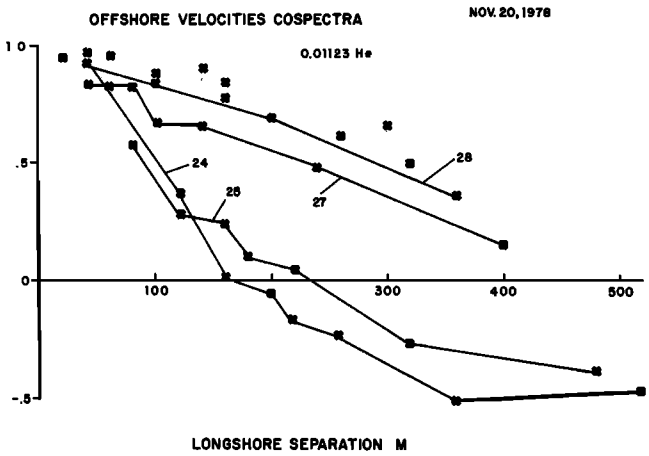

Fig. 11. Cospectra of on/offshore velocity at $f = 0.01123$ Hz plotted against longshore separation. Solid lines join data with sensor (24, 25, 27, or 28) in common for all cospectra. Data from November 20, 1978.

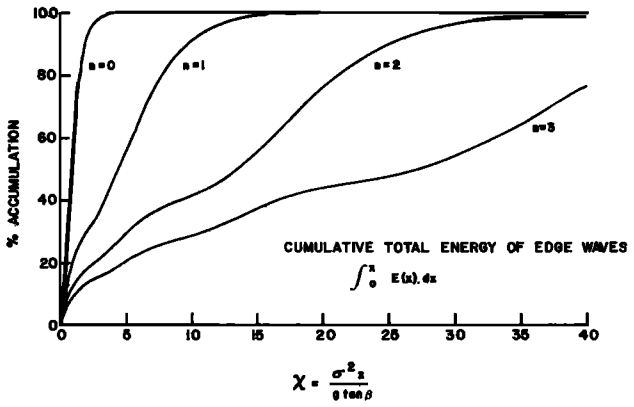

Fig. 12. Percentage of edge wave energy inshore of the nondimensional offshore distance χ, plotted against χ for edge wave modes 0 to 3.

TABLE 2. Frequencies at Which Edge Wave Energy Is Equally Divided Onshore and Offshore From $x = 275$ m (Assuming $\tan \beta = 0.02$)

Mode Number	Frequency, Hz
0	4.1×10^{-3}
1	9.0×10^{-3}
2	1.55×10^{-2}
3	2.19×10^{-2}

and 0.025 Hz. These results may be due to generation of the edge waves by narrow beam incident waves or may be some more general response of the nearshore zone to edge wave forcing. This question is being investigated using similar data sets collected under a variety of incident wave conditions. In any event, it seems probable that the ratio of the surf zone width to the offshore length scale of the edge waves plays an important role in controlling the frequency and mode number at which edge waves can exist.

For longshore currents, 30 ± 15% is a lower limit on the percentage of total energy at any given frequency which exists as progressive edge wave energy. The remaining energy is apparently randomly spread out to the Nyquist wave number, though there is a tendency for increased background energy toward $k = 0$. Other than this slight 'redness,' the background energy is probably the result of poor stability of the cross spectra used to form the two-dimensional energy spectrum, and this suggests that substantially more than 30% of the total longshore current energy is in fact in progressive edge waves.

Offshore profiles of the longshore current amplitude, measured using 10 sensors in an on/offshore line, are in good agreement with the predicted profiles.

The on/offshore currents present a rather different picture which, while not inconsistent with the longshore currents, suggests that other sources of energy than progressive edge waves are important to the on/offshore flow. One suggestion is that some of the edge wave energy is reflected, possibly by Scripps Canyon about 2.6 km to the south, and sets up standing waves at the array. This hypothesis is supported by cospectral measurements which clearly show that the low frequency wave climate is spatially inhomogeneous alongshore. These standing waves, if of high mode number ($n \geq 2$), would be much more important to on/offshore than to longshore velocities. Another contributor to differences between on/offshore and longshore surf beat velocities may be the forced long wave response to incident wave groups; for nearly normally incident waves this response will provide much stronger on/offshore currents than longshore currents. Both of these suggestions are the subject of further investigations.

Acknowledgments. The data discussed in this paper were collected during a large nearshore dynamics experiment funded by the Sea Grant National Sediment Transport Study and the Office of Naval Research. Data analysis was supported by the Office of Naval Research, Geography Branch, under contract number N000014-75-C-0300. D.A.H. also received support from the Natural Sciences and Engineering Research Council of Canada. The help of Steve Pawka in giving us access to his incident wave directional spectra and in aspects of the analysis is gratefully acknowledged. D.A.H. enjoyed the support and hospitality of the members of the Center for Coastal Studies at Scripps during a sabbatical in which the data analysis was begun.

REFERENCES

Bowen, A. J., and R. T. Guza, Edge waves and surf beat, *J. Geophys. Res., 83,* 1913–1920, 1978.

Bowen, A. J., and D. L. Inman, Rip currents, 2, Laboratory and field observations, *J. Geophys. Res., 74,* 5479–5490, 1969.

Bowen, A. J., and D. L. Inman, Edge waves and crescentic bars, *J. Geophys. Res., 76,* 8662–8671, 1971.

Davis, R. E., and L. Regier, Methods for estimating directional wave spectra from multi-element arrays, *J. Mar. Res., 35,* 453–477, 1977.

Eckart, C., Surface waves in water of variable depth, Wave Report, *SIO Ref. 51-12, 100,* 99 pp., Scripps Inst. Oceanogr., La Jolla, Calif., 1951.

Gallagher, B., Generation of surf beat by non-linear wave interactions, *J. Fluid Mech., 49,* 1–20, 1971.

Guza, R. T., and A. J. Bowen, The resonant instabilities of long waves obliquely incident on a beach, *J. Geophys. Res., 80,* 4529–4534, 1975.

Guza, R. T., and A. J. Bowen, Finite amplitude edge waves, *J. Mar. Res., 34*(1), 269–293, 1976.

Guza, R. T., and A. J. Bowen, Resonant interactions for waves breaking on a beach, *Proc. 16th Conf. Coastal Eng.,* 560–579, 1977.

Guza, R. T., and R. E. Davis, Excitation of edge waves by waves incident on a beach, *J. Geophys. Res., 79*(9), 1285–1291, 1974.

Guza, R. T., and D. L. Inman, Edge waves and beach cusps, *J. Geophys. Res., 80*(21), 2997–3012, 1975.

Guza, R. T., and E. B. Thornton, Local and shoaled comparisons of sea surface elevations, pressures and velocities, *J. Geophys. Res., 85,* 1524–1530, 1980.

Hasselmann, K., W. Munk, and G. MacDonald, Bispectra of ocean waves, in *Time Series Analysis,* edited by M. Rosenblatt, pp. 125–39. John Wiley, New York, 1963.

Holman, R. A., Infragravity waves on beaches, Ph.D. thesis, Dalhousie Univ., Halifax, N.S., Canada, 1979.

Holman, R. A., and A. J. Bowen, Edge waves on complex beach profiles, *J. Geophys. Res., 84,* 6339–6346, 1979.

Huntley, D. A., Long period waves on a natural beach, *J. Geophys. Res., 81,* 6441–6449, 1976.

Huntley, D. A., Edge waves on a crescentic bar system, The Coastlines of Canada, *Pap. 80-10,* pp. 111–121, Geological Society of Canada, 1980*a*.

Huntley, D. A., Morphodynamics of reflective and dissipative beach and inshore systems: Southeastern Australia, Comments, *Mar. Geol. 37,* 371–376., 1980*b*.

Inman, D. L., C. E. Nordstrom, and R. E. Flick, Currents in submarine canyons: An air-sea-land interaction, *Ann. Rev. Fluid Mech., 8,* 275–310, 1976.

Inman, D. L., and A. J. Bowen, Spectra of breaking waves, *Eos Trans. AGU, 48,* 146, 1967.

Longuet-Higgins, M. S., and R. W. Stewart, Radiation stress and mass transport in gravity waves, with application to "surf-beats," *J. Fluid Mech., 13,* 481–504, 1962.

Lowe, R. L., D. L. Inman, and B. M. Bush, Simultaneous data system for instrumenting the shelf, *Proc. 13th Conf. Coastal Eng.,* 95–112, 1972.

Mei, C. C., and L. F. Liu, The damping of surface gravity waves in a bounded liquid, *J. Fluid Mech., 59,* 239–256, 1973.

Munk, W., Surf beats, *Eos Trans. AGU 30,* 849–854, 1949.

Munk, W., F. Snodgrass, and F. Gilbert, Long waves on the continental shelf: An experiment to separate trapped and leaky modes, *J. Fluid Mech., 20,* 529–554, 1964.

Sasaki, T. O., and K. Horikawa, Observation of nearshore current and edge waves, *Proc 16th Conf. Coastal Eng.,* 791–809, 1979.

Suhayda, J. N., Standing waves on beaches, *J. Geophys. Res., 79,* 3065–3071, 1974.

Tucker, M. J., Surf beats: Sea waves of 1 to 5 min period, *Proc Roy. Soc., Ser. A, 202,* 565–573, 1950.

Ursell, F., Edge waves on a sloping beach, *Proc. Roy. Soc. Ser. A, 214,* 79–98, 1952.

Wright, L. D., J. Chappell, B. G. Thom, M. P. Bradshaw, and P. Cowell, Morphodynamics of reflective and dissipative beach and inshore systems. Southeastern Australia, *Mar. Geol. 32,* 105–140, 1979.

(Received September 5, 1980;
revised March 26, 1981;
accepted March 31, 1981.)